Spin properties of quantum wells with magnetic barriers. I. A k·p analysis for structures with normal band ordering

N. Malkova
Institute of Applied Physics, AS of Moldova, 2028 Kishinev, Moldova, and Department of Microelectronics and Information Technology, Royal Institute of Technology, SE-164 40 Kista, Sweden

U. Ekenberg
Department of Microelectronics and Information Technology, Royal Institute of Technology, SE-164 40 Kista, Sweden
(Received 4 May 2001; revised manuscript received 18 June 2002; published 29 October 2002)

The electronic band-edge spectrum of magnetic semiconductor quantum wells containing a diluted magnetic semiconductor as one of the constituents is studied within the envelope-function formalism. The effects of Mn *d* electrons are explicitly included in a $\mathbf{k}\cdot\mathbf{p}$ Hamiltonian which in the first approximation of perturbation theory is shown to be reduced to an effective Kane model. The *sp-d* hybridization leads to a spin-splitting effect. The results are applied to the system $Cd_{1-x}Mn_xTe/CdTe$. The spin-splitting effect is studied as a function of external magnetic field, well width, valence band offset and fraction of the magnetic atoms. The numerical results are in accord with experimental data.

DOI: 10.1103/PhysRevB.66.155324 PACS number(s): 73.20.At, 75.70.Cn

I. INTRODUCTION

The experimental and theoretical studies of quantum confinement of carriers in spatially modulated semiconductor structures have been a field of intense activity over the past decades. Magnetic semiconductor quantum wells and superlattices are relatively new in this context. The incorporation of magnetic impurities into semiconductor heterostructures combines magnetism and quantum-size effects to produce exotic new physics. Such semiconductors are commonly called dilute magnetic semiconductors or semimagnetic semiconductor. For simplicity we will refere to quantum wells containing magnetic impurities as magnetic quantum wells. Von Ortenberg[1] seems to have been the first to propose that a magnetic field could be used to induce a spin-dependent potential in a magnetic semiconductor heterostructure to form a ''spin superlattice'' consisting of spatially separated spin states. A direct experimental evidence of spin superlattices was given in Refs. 2 and 3. The essential idea of the spin-dependent phenomena in magnetic semiconductors is that electrons interact with the *d* or *f* electrons of the localized magnetic moments of the magnetic ions through the exchange potential. In an external magnetic field this interaction gives rise to a giant effective Zeeman effect which lifts the degeneracy of the spin-up and spin-down electron and hole states.

This effect has renewed the interest in the magnetic semiconductor heterostructures in connection with their utilization in a new field of electronics—spin electronics or ''spintronics''—where both the charge and spin of the electron are exploited as an active element of electron devices.[4] Nowadays the application of magnetic semiconductor heterostructures in spin electronics is considered in two main systems. One concerns field effect transistors or light-emitting diodes in which the magnetic semiconductor has the role of a spin-aligning material. The problem is that in spite of tremendous interest in spin-polarized electron injection into semiconductors as one of the most important elements of the spin transistor[5] the experiments for spin injection from ferromagnetic metals into semiconductors have only given effects of less than 1% (Ref. 6). The basic obstacle for spin injection from a ferromagnetic metallic emitter into a semiconductor has been recently been shown[7] to originate from the conductivity mismatch between these materials. In order to avoid this mismatch it has been suggested to replace the metal contacts with magnetic semiconductors using their large Zeeman splitting. The experiments[8–10] on the circular polarization of the electroluminescence showed that the electron spin polarization of such magnetic structures was almost 90%. Another application of magnetic semiconductor heterostructures follows from a spin-dependent resonant tunneling effect based on von Ortenberg's idea as well. It was suggested[11–14] to use a magnetic-field tunable $ZnSe/Zn_{1-x}Mn_xSe$ heterostructure as a spin filter. It is worth mentioning another possible application of the magnetic tunneling structures combining the first two points. It was recently shown by Rashba[15] that including a tunnel contact at the interface between a ferromagnetic metal and normal semiconductor can solve the problem of the large conductivity mismatch of these materials. These structures show a strong spin polarization effect and in this way they are promising for spin electronics.

Spin electronic devices are commonly based on the well determined and carefully controlled spin-splitting effect of the two-dimensional electron gas. It is now recognized that the splitting in asymmetric quantum wells based on zinc blende III-V or II-VI semiconductors has two distinct contributions[16–18] even in the absence of an applied magnetic field and magnetic ions. One contribution is due to inversion asymmetry of the bulk host material.[19,20] The other one stems from the asymmetry of the macroscopic confining potential being derived from general symmetry arguments. It is commonly called the Rashba effect[21] and is the proposed mechanism behind the spin transistor.[5] The Rashba term results from the relativistic effect in which a moving electron

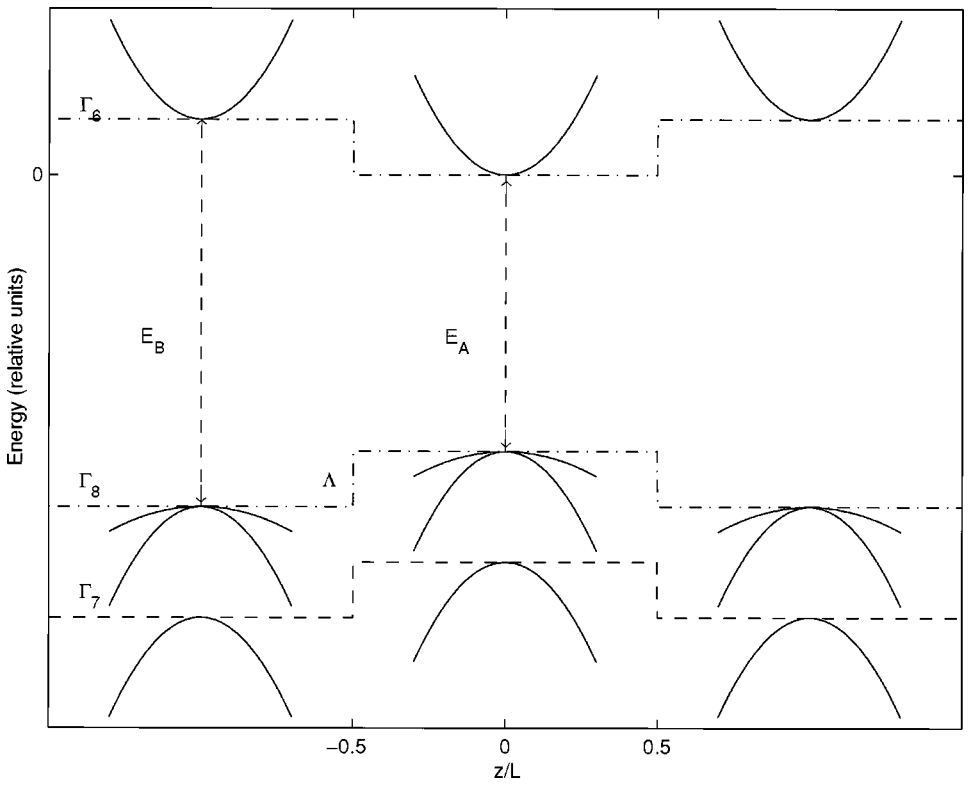

FIG. 1. Schematic band diagram for the quantum well $CdTe/Cd_{1-x}Mn_xTe/CdTe/$ studied. In each material the conduction band (Γ_6), the heavy-hole and the light-hole bands (Γ_8), and the spin-orbit split-off band (Γ_7) are displayed from top to bottom together with symmetry notations, band gaps, and valence-band offset Λ.

with nonzero wave vector **k** in its reference frame sees the interface electric field transformed into a magnetic field.[22]

In the magnetic semiconductor heterostructures another spin-splitting effect must be taken into consideration. This is the spin-dependent exchange potential[1] mentioned above which gives rise to the ''spin superlattices.'' This exchange term in the spin-splitting effect of the magnetic structures is clearly dominant since the first two terms are equal to zero in the first order of perturbation theory.

In this work we are dealing with the theoretical analysis of the spin-splitting effect of the magnetic semiconductor heterostructures. We are interested in magnetic semiconductor quantum wells based on II-VI semiconductors. Quantum wells of the type $A^{II}_{1-x}Mn_xB^{VI}/A^{II}B^{VI}/A^{II}_{1-x}Mn_xB^{VI}$ are considered as model materials and heterostructures with normal and inverted band arrangement are studied. (Here A^{II} is one of the group II elements and B^{VI} is a group VI element). We study $Cd_{1-x}Mn_xTe/CdTe$ as an example of the structure with the normal band arrangement (see Fig. 1) in the first part of this paper and the quantum well $Hg_{1-x}Mn_xTe/HgTe$ as an example of the structure with the inverted band structure in the following part[23] of this sequence of papers. As a first step in our investigation we study a symmetrical square quantum well in the approximation of flat bands and neglect strain effects. Thus, the asymmetry effect coming from the Rashba spin splitting terms is absent. Moreover, as a first approximation of the model, we neglect the bulk asymmetry effect (Dresselhaus term). The only spin-splitting potential, which will be included in the Hamiltonian, is the spin-dependent interaction between the bare sp electrons and the d electrons of Mn. It is important to note that for magnetic semiconductor structures even for an asymmetric quantum well potential the mentioned two spin-splitting terms will result in small corrections compared to the exchange splitting.

The bulk band Hamiltonian for the magnetic semiconductor is constructed in the framework of a model developed earlier.[24–26] Starting from the microscopic theory of the bulk magnetic II-VI semiconductors,[27] P.M. Hui *et al.*[24] have suggested an ''effective'' sp-band Hamiltonian model, which then has been applied to magnetic II-VI superlattices.[25] We are extending this approach to the case of the magnetic II-VI quantum wells. The structural and electronic similarities between the constituents allows us to use the envelope function approximation when considering the quantum well states.

In order to simulate the effects of the externally applied magnetic field, in the above model[24] a spin polarization was included at the outset. In principle one can in this way encompass the possibility of ferromagnetic materials, but in this paper we will mainly consider the spin polarization resulting from an external magnetic field. This approach, initially suggested in Refs. 28 and 29, is based on the itinerent model of the semimagnetic semiconductors which extends the Anderson impurity theory. Up to 70 % of Mn the (Cd-,Mn)Te alloy retains the zinc blende structure with randomly occupied cationic sites. The magnetic moment orientation at each site varies randomly in time; this makes the system paramagnetic. The simplest itinerant representation of magnetic disorder is defined by Ising model, that is, (i) neglect of intersite correlations, (ii) static limit, (iii) limiting the spin orientation to two opposing directions ($\uparrow$ and $\downarrow$).[30] Thus, the magnetic semiconductor alloy can be presented as an effective ternary system $A^{II}_{1-x}Mn^{\uparrow}_{xy}Mn^{\downarrow}_{x(1-y)}B^{VI}$. In this approach the parameter y gives the value of the polarization of the magnetic atoms $P=(N^{\uparrow}-N^{\downarrow})/(N^{\uparrow}+N^{\downarrow})=2y-1$. Here $N^{\uparrow}(N^{\downarrow})$ is the number of Mn ions with spin up (down) which

may be changed, for example, by an external magnetic field or by the temperature. For the unpolarized material $y=1/2$ and in the case of finite spin polarization $y\neq 1/2$. Thus, the magnetic field effect on the band spectrum of the spin-polarized magnetic structures is implicitly included in the model through the parameter y. We ignore the effects of the Landau level quantization and the ordinary Zeeman splitting. In the spin-polarized alloy the sp-d hybridization was shown[25] to lead to an effective sp Hamiltonian having the same form as the usual mean field exchange Hamiltonian for the magnetic semiconductors. This approach proved to be very effective in explaining the kinetics and optical experimental data. The electron effective masses and gaps as well as the fundamental absorption coefficients calculated in the framework of this model for a number of II-VI and III-V semiconductor superlattices are shown to be in excellent agreement with experimental data.[26] It is also important to note that because of its simplicity the model gives analytical results and thus simplifying the interpretation of the physical effects.

The paper is organized as follows. In Sec. II we describe our theoretical model. The band-edge spectrum and the wave functions for the magnetic quantum well structures are obtained. The spin-splitting effect is discussed and the spin properties of the electron and hole states are studied. In Sec. III these results are applied to the quantum well $Cd_{1-x}Mn_xTe/CdTe/Cd_{1-x}Mn_xTe$ which is an extensively studied magnetic structure. In Sec. IV a discussion of the results follows and section V concludes the paper with a summary of the main results.

II. MODEL HAMILTONIAN

Our problem now is to get the band-edge spectrum and wave functions of the square quantum well incorporating the magnetic semiconductor. As discussed above we neglect strain, Landau level quantization, and Zeeman splitting. Then the fundamental Hamiltonian for the $A^{II}_{1-x}Mn_xB^{VI}$ magnetic semiconductor is written in the form[24]

$$H=H^0_{sp}+H^0_d+H_{sp\text{-}d}, \tag{1}$$

where H^0_{sp} describes the unperturbed sp valence and conduction bands, H^0_d is the Hamiltonian of the Mn d states, and $H_{sp\text{-}d}$ includes the hybridization between the d states and the sp bands. Since the quantum structure is considered with the growth direction along the z axis, all these terms are step functions of z. We suppose that $z=0$ defines the center of the well layer. A schematic band diagram for the quantum well $Cd_{1-x}Mn_xTe/CdTe/Cd_{1-x}Mn_xTe$ is shown in Fig. 1.

In the envelope function approximation the wave function is expanded in the periodic parts of bulk Bloch functions of the constituents at the zone center ($\mathbf{k}=0$)

$$\Psi(\mathbf{r})=e^{\mathbf{i}\cdot\mathbf{k}_\perp\cdot\mathbf{r}_\perp}\left(\sum_{\mathbf{i}=1}^{8}\mathbf{f}_i(\mathbf{z})|\mathbf{s}p_i\rangle+\sum_{\nu,\mathbf{j}=1}^{6}\varphi^\nu_j(\mathbf{z})|\mathbf{d}^\nu_j\rangle\right). \tag{2}$$

Here $\mathbf{k}_\perp=(k_x,k_y)$ and $\mathbf{r}_\perp=(x,y)$ are the two-component wave vector and position vector, respectively, in the interface plane, $f_i(z)$ and $\varphi^\nu_j(z)$ are the slowly varying envelope functions, and $|sp_i\rangle,|d^\nu_j\rangle$ are the basis Bloch functions for the H^0_{sp} and H^0_d Hamiltonians, respectively. The index $\nu=v$ or c denotes the occupied ''valence'' or unoccupied ''conduction'' d states, respectively.

We include the spin-orbit interaction and the basis functions $|sp_i\rangle$ used are taken in the form[31]

$$|sp_1\rangle=|S\uparrow\rangle,$$

$$|sp_2\rangle=|S\downarrow\rangle,$$

$$|sp_3\rangle=\sqrt{\frac{2}{3}}|Z\uparrow\rangle-\sqrt{\frac{1}{6}}(|X\downarrow\rangle+i|Y\downarrow\rangle),$$

$$|sp_4\rangle=\sqrt{\frac{2}{3}}|Z\downarrow\rangle+\sqrt{\frac{1}{6}}(|X\uparrow\rangle-i|Y\uparrow\rangle),$$

$$|sp_5\rangle=\sqrt{\frac{1}{2}}(|X\uparrow\rangle+i|Y\uparrow\rangle),$$

$$|sp_6\rangle=\sqrt{\frac{1}{2}}(|X\downarrow\rangle-i|Y\downarrow\rangle),$$

$$|sp_7\rangle=\sqrt{\frac{1}{3}}(|Z\uparrow\rangle+|X\downarrow\rangle+i|Y\downarrow\rangle),$$

$$|sp_8\rangle=\sqrt{\frac{1}{3}}(|Z\downarrow\rangle-|X\uparrow\rangle+i|Y\uparrow\rangle). \tag{3}$$

Here $S\sigma$ is the s-symmetric, spin σ state associated with the conduction band edge, while the p-symmetric functions $|X\sigma\rangle,|Y\sigma\rangle,|Z\sigma\rangle$ are the valence band Bloch functions. In this basis at $\mathbf{k}=(0,0,k)$ the envelope-function equation for the Hamiltonian H^0_{sp} has the usual Kane[31,32] form

$$\begin{pmatrix} [\varepsilon_c^0(z)-E]I & \frac{iP\hbar k_z}{m}I & 0 & \frac{iP\hbar k_z}{\sqrt{2}m}I \\ -\frac{iP\hbar k_z}{m}I & [\varepsilon_v^0(z)-E]I & 0 & 0 \\ 0 & 0 & \left[\varepsilon_v^0(z)-\frac{\hbar^2}{2}k_z\frac{1}{m_{hh}(z)}k_z-E\right]I & 0 \\ -\frac{iP\hbar k_z}{\sqrt{2}m}I & 0 & 0 & (\varepsilon_{so}^0(z)-E)I \end{pmatrix} \mathbf{f}=0. \tag{4}$$

Here $\mathbf{f}$ is the column vector with the components f_i. For layered structures the z component of the momentum operator k_z is replaced by $=-i\partial/\partial z$. I is the 2×2 unit matrix, which appears since each energy level of the symmetrical structure is doubly Kramers degenerate. We define $\varepsilon_c^0(z)$, $\varepsilon_v^0(z)$, $\varepsilon_{so}^0(z)$, as the z-dependent bare sp band energies at $\mathbf{k}=0$ for the Γ_6 conduction band, the Γ_8 degenerate hole band and the Γ_7 spin-orbit split-off band, respectively. The origin of energy is defined as the Γ_6 edge of the well material. $P=-i\sqrt{2/3}\langle S\sigma|p_z|Z\sigma\rangle$ is the usual Kane matrix element. The function $m_{hh}(z)$ corresponds to the heavy-hole mass, which varies between the materials along the z direction.

As explained in the Introduction, using the assumption that the Mn local moments are Ising-like, we divide all of the Mn ions into two species, namely, into ions with spin up $\mathrm{Mn}^{\uparrow}$ and into ions with spin down $\mathrm{Mn}^{\downarrow}$. Thus, the magnetic semiconductor alloy can be presented in the form $A^{\mathrm{II}}_{1-x}\mathrm{Mn}^{\uparrow}_{xy}Mn^{\downarrow}_{x(1-y)}B^{\mathrm{VI}}$. From this assumption in the frame of the tight binding model the basis functions of the H_d^0 Hamiltonian at $\mathbf{k}=0$ are written as

$$|d_i^{\nu}\rangle=\sqrt{\frac{1}{N_{\nu\sigma l,(\nu\sigma)}}}\sum \phi_i(\mathbf{r}-\mathbf{R}_l)\sigma. \tag{5}$$

Here $N_{\nu\sigma}$ is a normalization constant, equal to Nxy for $(\nu,\sigma)=(v,\uparrow)$ or $(c,\downarrow)$ and equal to $Nx(1-y)$ for $(\nu,\sigma)=(v,\downarrow)$ or $(c,\uparrow)$; N is the total number of the cation sites. ϕ_i are linear combinations of the atomic d functions which are assumed to form an orthonormal set and to be orthogonal to the sp basis functions (3). Following the results of Ref. 24 we pick ϕ_i in the form

$$|\phi_1\rangle=\sqrt{\frac{2}{3}}|d_{xy}\uparrow\rangle-\sqrt{\frac{1}{6}}(|d_{yz}\downarrow\rangle+i|d_{zx}\downarrow\rangle),$$

$$|\phi_2\rangle=\sqrt{\frac{2}{3}}|d_{xy}\downarrow\rangle+\sqrt{\frac{1}{6}}(|d_{yz}\uparrow\rangle-i|d_{zx}\uparrow\rangle),$$

$$|\phi_3\rangle=\sqrt{\frac{1}{2}}(|d_{yz}\uparrow\rangle+i|d_{zx}\uparrow\rangle),$$

$$|\phi_4\rangle=\sqrt{\frac{1}{2}}(|d_{yz}\downarrow\rangle-i|d_{zx}\downarrow\rangle),$$

$$|\phi_5\rangle=\sqrt{\frac{1}{3}}(|d_{xy}\uparrow\rangle+|d_{yz}\downarrow\rangle+i|d_{zx}\downarrow\rangle),$$

$$|\phi_6\rangle=\sqrt{\frac{1}{3}}(|d_{xy}\downarrow\rangle-|d_{yz}\uparrow\rangle+i|d_{zx}\uparrow\rangle). \tag{6}$$

Making use of Ising-like properties of the Mn local moments (that is, neglecting the Mn d states overlapping with neighboring Mn sites and their spin-orbital interaction), in the basis (6) we can write the quantum well envelope-function equation for the Hamiltonian H_d^0 in a diagonal (12×12) form with the matrix elements ε_d for the ''valence'' bands and ε_d+U for the ''conduction'' bands, where ε_d is the energy of the occupied d state and U is an effective exchange-correlation parameter describing, in terms of the Anderson model, the energy changes when adding an additional d electron to a Mn site.

By symmetry no s-d hybridization is allowed. (This can be easily checked up by direct calculation with the basis functions $|S\sigma\rangle$ and $|\phi_i\rangle$). The rest part of the p-d hybridization Hamiltonian $H_{pd}^{\nu}=\langle sp|H|d^{\nu}\rangle$ can be written in the chosen basis as a sum of two matrices

$$H_{pd}^{\nu}=V^{\nu}+\Pi^{\nu}. \tag{7}$$

The matrix V^v has the form[24]

$$V^v=\begin{pmatrix} B & 0 & 0 & 0 & D & 0 \\ 0 & C & 0 & 0 & 0 & -D \\ 0 & 0 & E & 0 & 0 & 0 \\ 0 & 0 & 0 & F & 0 & 0 \\ D & 0 & 0 & 0 & C & 0 \\ 0 & -D & 0 & 0 & 0 & B \end{pmatrix} =\begin{pmatrix} V_v^{11} & 0 & V_v^{13} \\ 0 & V_v^{22} & 0 \\ V_v^{13} & 0 & V_v^{33} \end{pmatrix}. \tag{8}$$

The matrix elements involved are defined by the relations

$$B=\frac{4}{3}V_{pd}\sqrt{x}(2\sqrt{y}+\sqrt{1-y}),$$

$$C=\frac{4}{3}V_{pd}\sqrt{x}(2\sqrt{1-y}+\sqrt{y}),$$

$$D=\frac{4}{3}V_{pd}\sqrt{x}\sqrt{2}(\sqrt{y}-\sqrt{1-y}),$$

$$E=4V_{pd}\sqrt{xy},$$

$$F=4V_{pd}\sqrt{x(1-y)}, \tag{9}$$

where $V_{pd}=(1/\sqrt{2})\langle X\uparrow|H|d_{yz}\uparrow\rangle$ is the matrix element of the p-d hybridization. [In Eq. (8) we display the 2×2 matrices V_v^{ij} to simplify the future mathematical manipulations.] The matrix Π is k-dependent and in the case of $\mathbf{k}=(0,0,k)$ it is given by

$$\Pi^v=\sqrt{x}\Pi_{pd}k\begin{pmatrix} 0 & 0 & 0 & -\sqrt{\frac{1-y}{3}} & 0 & 0 \\ 0 & 0 & -\sqrt{\frac{y}{3}} & 0 & 0 & 0 \\ 0 & \sqrt{\frac{y}{3}} & 0 & 0 & 0 & -\sqrt{\frac{2y}{3}} \\ \sqrt{\frac{1-y}{3}} & 0 & 0 & 0 & -\sqrt{\frac{2(1-y)}{3}} & 0 \\ 0 & 0 & 0 & \sqrt{\frac{2(1-y)}{3}} & 0 & 0 \\ 0 & 0 & \sqrt{\frac{2y}{3}} & 0 & 0 & 0 \end{pmatrix}, \tag{10}$$

where $\Pi_{pd}=(1/\sqrt{2})\langle X\uparrow|H|d_{xy}\uparrow\rangle$. The matrices V^c and Π^c, describing the hybridization between the p and unoccupied d^c states, have the similar forms but with mutual replacement $\sqrt{y}\leftrightarrow\sqrt{1-y}$. It worth noting that in the general case when $\mathbf{k}=(k_x,k_y,k_z)$, the matrices Π^v include $\mathbf{k}_\perp$-dependent terms which look similar to the Rashba terms and result in the similar effect. We emphasize that these terms, which are related to the large exchange potential, can have a larger effect on the spin-splitting of the in-plane dispersion than the Rashba effect originating from the possibility of inversion asymmetry of the quantum well structure.

Now we use the method of finding the formal transformation $\mathbf{U}$ which diagonalizes the Hamiltonian at $\mathbf{k}=0$. We note that in the unpolarized case ($y=1/2$) due to the chosen basis, Eqs. (3) and (6), each $|sp_i\rangle$ function hybridizes by the $V_{c,v}^{ii}$ only with the $|d_i^{c,v}\rangle$ functions with just the same value of i. In the spin-polarized case, the matrices $V^{c,v}$ are not diagonal and $V_{c,v}^{13}$ blocks couple the $|sp_i\rangle$ and $|d_j\rangle$ functions with different indices i and j. By rearranging the basis functions in the sequence $|sp_{3,4}\rangle$, $|d_{3,4}^v\rangle$, $|d_{3,4}^c\rangle$; $|sp_{5,6}\rangle$, $|d_{5,6}^v\rangle$, $|d_{5,6}^c\rangle$; $|sp_{7,8}\rangle$, $|d_{7,8}^v\rangle$, $|d_{7,8}^c\rangle$, we rewrite the H_{pd} Hamiltonian matrix in the form

$$H_{pd}=\begin{pmatrix} H_{pd}^{11} & 0 & H_{pd}^{13} \\ 0 & H_{pd}^{22} & 0 \\ H_{pd}^{31} & 0 & H_{pd}^{33} \end{pmatrix}. \tag{11}$$

Here all diagonal matrices have identical form

$$H_{pd}^{ii}=\begin{pmatrix} \varepsilon_i^0 I & V_v^{ii} & V_c^{ii} \\ V_v^{ii} & \varepsilon_d^0 I & 0 \\ V_c^{ii} & 0 & (\varepsilon_d^0+U)I \end{pmatrix},$$

where $\varepsilon_i^0=\varepsilon_v^0$ for $i=1,2$ and $\varepsilon_i^0=\varepsilon_{so}^0$ for $i=3$. The off-diagonal blocks are written as

$$H_{pd}^{13}=\begin{pmatrix} 0 & V_v^{13} & V_c^{13} \\ V_v^{13} & 0 & 0 \\ V_c^{13} & 0 & 0 \end{pmatrix}.$$

Thus the transformation $\mathbf{U}$ which makes the matrix $\tilde{H}_{pd}=\mathbf{U}^+H_{pd}\mathbf{U}$ diagonal can be written in the form

$$\mathbf{U}=\begin{pmatrix} U^{11} & 0 & U^{13} \\ 0 & U^{22} & 0 \\ U^{31} & 0 & U^{33} \end{pmatrix}. \tag{12}$$

Now in the new basis $\mathbf{U}^+\Psi$, we construct a new effective $\mathbf{k}\cdot\mathbf{p}$ Hamiltonian. The resulting ''folded down'' effective sp Hamiltonian has the form

$$H_{sp}=\begin{pmatrix} \varepsilon_c(z)I & \frac{iP\hbar k_z}{m}I & 0 & \frac{iP'\hbar k_z}{\sqrt{2}m}I \\ -\frac{iP\hbar k_z}{m}I & \hat{\varepsilon}_{v1}(z) & k_z\hat{P}'_{pd} & \hat{V}_{pd} \\ 0 & -k_z\hat{P}'_{pd} & \hat{\varepsilon}_{v2}(z)-\frac{\hbar^2}{2}k_z\frac{1}{m_{hh}(z)}\hat{k}_zI & k_z\hat{P}_{pd} \\ -\frac{iP'\hbar k_z}{\sqrt{2}m}I & \hat{V}_{pd} & k_z\hat{P}_{pd} & \hat{\varepsilon}_{so}(z) \end{pmatrix}. \tag{13}$$

Here all the matrices $\hat{\varepsilon}_{v1}$, $\hat{\varepsilon}_{v2}$, and $\hat{\varepsilon}_{so}$ have the identical form

$$\hat{\varepsilon}_{vi,so}(z)=\begin{pmatrix} \varepsilon_{v,so}-(2/3)(v_{i,so}\sqrt{y}+v'_{i,so}\sqrt{1-y}) & 0 \\ 0 & \varepsilon_{v,so}-(2/3)(v_{i,so}\sqrt{1-y}+v'_{i,so}\sqrt{y}), \end{pmatrix},$$

while the offdiagonal matrices are given by

$$\hat{P}_{pd}=P_{pd}\begin{pmatrix} 0 & p_{22}\sqrt{y}+p'_{22}\sqrt{1-y} \\ p_{22}\sqrt{1-y}+p'_{22}\sqrt{y} & 0 \end{pmatrix},$$

$\hat{P}'_{pd}=-iP_{pd}p_{11}(\sqrt{y}-\sqrt{1-y})\sigma_y$, $\hat{V}_{pd}=V_{pd}v_{13}(\sqrt{y}-\sqrt{1-y})\sigma_z$.

Here the Kane sp parameters ε_v, ε_{so}, P' are renormalized by the $p-d$ hybridization, the parameters $v_{i,so}$, $v'_{i,so}$, p_{ij} are determined by the transformation matrix $\mathbf{U}$, and $\sigma_{x,y,z}$ are the Pauli matrices.

It follows from the form of the Hamiltonian H_{sp} (13) that the magnetic semiconductor structure can be described by a modified Kane model in which some new blocks have been included. All the valence bands are split by the p-d hybridization while the conduction bands are still doubly degenerate because of the vanishing matrix elements $\langle S\sigma|H|d_i\rangle$. This reflects the different symmetry character of the conduction- and valence-band edges, which results in the qualitative difference between the valence- and conduction-band-edge spin splittings. The much smaller value of the conduction band spin-splitting, moreover directed in the opposite direction, has been shown by a microscopic model in Ref. 27, to be determined exclusively by the exchange potential. In the mean-field approximation the exchange potential is well known to be written as

$$H_{ex}=x\sigma_z\langle S_z\rangle\sum_i J(\mathbf{r}-\mathbf{R}_i), \tag{14}$$

where $\mathbf{R}_i$ are the cation sites and $\langle S_z\rangle=\frac{5}{2}(2y-1)$ is the average value of the Mn spin. By using the basis functions $|S\sigma\rangle$ and $|d_i\rangle$, we immediately obtain the exchange correction to the conduction bands which is equal to $\langle S\sigma|H_{ex}|d_i\rangle=x\langle S_z\rangle(N_0\alpha)\sigma_z$ [where $(N_0\alpha)=N_0\langle S\uparrow|J|S\uparrow\rangle$, N_0 is the number of the cation sites per unit volume].

We note that there is a difference between the matrix H_{sp} (13) and the resulting Hamiltonian in Ref. 24. In the matrix H_{sp}, there appear k-dependent terms proportional to $(\sqrt{y}-\sqrt{1-y})$, which correspond to the spin-polarized case. These terms were omitted in Ref. 24, but for more careful examination of the spin-splitting effect they will surely give rise to additional peculiarities of the spectrum.

Another solution of the problem can be obtained in the framework of perturbation theory in which the Hamiltonian $H_{sp\text{-}d}$ is considered as a perturbation. This is reasonable taking into account the large energy separation between sp and d states ($\sim 3-7$ eV) in comparison with energies of the sp bands. Using perturbation theory, we construct an effective 8×8 $\mathcal{H}_{sp}$ Hamiltonian by folding the full matrix down into the sp-block and keeping the terms to the order xV_{pd}^2. (See Ref. 31). One obtains

$$\mathcal{H}_{sp}=\begin{pmatrix} \hat{\epsilon}_c(z) & \frac{iP\hbar k_z}{m}I & 0 & \frac{iP'\hbar k_z}{\sqrt{2}m}I \\ -\frac{iP\hbar k_z}{m}I & \hat{\epsilon}_{v1}(z) & 0 & \hat{\mathcal{V}}_{pd} \\ 0 & 0 & \hat{\epsilon}_{v2}(z)+\frac{\hbar^2}{2}k_z\frac{1}{m_{hh}(z)}k_zI & k_z\hat{\mathcal{P}}_{pd} \\ -\frac{iP'\hbar k_z}{\sqrt{2}m}I & \hat{\mathcal{V}}_{pd} & k_z\hat{\mathcal{P}}_{pd} & \hat{\epsilon}_{so}(z) \end{pmatrix}. \tag{15}$$

The diagonal blocks of the Hamiltonian matrix are defined by the expressions

$$\hat{\epsilon}_c(z)=\varepsilon_c^0 I+x\langle S_z\rangle(N_0\alpha)\sigma_z,$$

$$\hat{\epsilon}_{v1}(z)=(\varepsilon_v^0+\delta\varepsilon_v)I-\frac{x}{6}\langle S_z\rangle(N_0\beta)\sigma_z;$$

$$\hat{\epsilon}_{v2}(z)=(\varepsilon_v^0+\delta\varepsilon_v)I-\frac{x}{2}\langle S_z\rangle(N_0\beta)\sigma_z;$$

$$\hat{\epsilon}_{so}(z)=(\varepsilon_{so}^0+\delta\varepsilon_{so})I+\frac{x}{6}\langle S_z\rangle(N_0\gamma)\sigma_z. \tag{16}$$

The offdiagonal blocks resulting from the spin-polarization effect are presented as

$$\hat{\mathcal{V}}_{pd}=-\frac{x\sqrt{2}}{3}\langle S_z\rangle\frac{(N_0\gamma)+(N_0\beta)}{2}\sigma_z; \tag{17}$$

$$\hat{\mathcal{P}}_{pd}=AP_{pd}\sigma_x. \tag{18}$$

Here the values

$$\delta\varepsilon_{v,so}=8xV_{pd}^2\left(\frac{1}{\varepsilon_{v,so}^0-\varepsilon_d}+\frac{1}{\varepsilon_{v,so}^0-\varepsilon_d-U}\right) \tag{19}$$

determine the shifts of the sp bands by the $p-d$ hybridization in the unpolarized case, and

$$(N_0\beta)=-\frac{32}{5}V_{pd}^2\left(\frac{1}{\varepsilon_v^0-\varepsilon_d}-\frac{1}{\varepsilon_v^0-\varepsilon_d-U}\right),$$

$$(N_0\gamma)=-\frac{32}{5}V_{pd}^2\left(\frac{1}{\varepsilon_{so}^0-\varepsilon_d}-\frac{1}{\varepsilon_{so}^0-\varepsilon_d-U}\right), \tag{20}$$

correspond to the energy correction in the spin-polarized case. The parameter A is a constant defined by the matrix elements of the transformation matrix $\mathbf{U}$ (Ref. 24).

By comparing the matrices H_{sp} (13) and $\mathcal{H}_{sp}$ (15) obtained by the two approaches we note that the difference between them is to include the spin-polarization effects in the k-dependent terms in H_{sp}. So, in the unpolarized case when $y=1/2$ we have $\hat{P}_{pd}\sim\sigma_x$ and $\hat{P}'_{pd}=0$. As a result, by symmetry the matrices H_{sp} and $\mathcal{H}_{sp}$ become identical provided the matrix elements involved are interpreted as empirical parameters. As a first step in the analysis of the magnetic structures we use the perturbation theory Hamiltonian $\mathcal{H}_{sp}$. Moreover, in order to avoid the complicated boundary conditions and to get an analytical result we neglect the offdiagonal blocks $\mathcal{P}_{pd}$ reducing the envelope function equation to an effective Kane model with renormalized matrix elements and the additional block $\mathcal{V}_{pd}$. We emphasize that this simplification is caused by our aim to understand the physics of the effect at first. However for a quantitative description of the quantum structures the full Hamiltonian H_{sp} should be considered.

III. SPIN-SPLITTING EFFECT FOR THE QUANTUM WELL STATES

Now we treat the quantum well problem and set $k_z=-i(\partial/\partial z)$. The envelope function equation

$$\mathcal{H}_{sp}\mathbf{f}=\mathbf{E}\mathbf{f} \tag{21}$$

is reduced to two sets of three coupled differential equations for the envelopes f_i^{lp} of the light particles (electrons, light holes, and split-off holes) and to two second order differential equations for the heavy hole envelopes f_i^{hh}. The envelope function boundary conditions resulting from integration of the equations across an interface require continuity of the envelopes $f_i^{lp,hh}$ and $(1/m_{hh})(\partial f_i^{hh}/\partial z)$.

The quantum well states have either even or odd parity under $\mathbf{r}\rightarrow-\mathbf{r}$ within the present symmetrical model. Therefore each quantum well state can be labeled by the parity. As a result, the following dispersion relations for the even states of the light particles and heavy holes are obtained:[33]

$$\cos k_{lp}L/2=-\frac{\kappa_{lp}^{\pm}}{k_{lp}}\frac{E}{E-\delta\varepsilon_c^{\pm}}\sin k_{lp}L/2, \tag{22}$$

$$\cos k_{hh}L/2=-\frac{\kappa_{hh}^{\pm}}{k_{hh}}\frac{m_{hh}^a}{m_{hh}^b}\sin k_{hh}L/2. \tag{23}$$

For the odd modes one gets

$$\sin k_{lp}L/2=\frac{\kappa_{lp}^{\pm}}{k_{lp}}\frac{E}{E-\delta\varepsilon_c^{\pm}}\cos k_{lp}L/2, \tag{24}$$

$$\sin k_{hh}L/2=\frac{\kappa_{hh}^{\pm}}{k_{hh}}\frac{m_{hh}^a}{m_{hh}^b}\cos k_{hh}L/2. \tag{25}$$

Here k_{lp} and k_{hh} are the bulk wave vectors in the well for the light particles and heavy holes, respectively; $i\kappa_{lp}^{\pm}$ and $i\kappa_{hh}^{\pm}$ are the bulk wave vectors in the two spin-split bands of the magnetic barriers; $\delta\varepsilon_c^{\pm}=\varepsilon_c^0(\pm\infty)\pm x\langle S_z\rangle(N_0\alpha)$; L is the width of the well. The bulk wave vectors of the constituents at given energy E are determined by the requirement $\det(\mathcal{H}_{sp}-E)=0$, where the coordinate dependent terms should be replaced by the corresponding constant values. So, for the light particles in the well and in the barriers we have, respectively,

$$\begin{vmatrix} \varepsilon_{ca}^0-E & \frac{iP\hbar k_{lp}}{m} & \frac{iP\hbar k_{lp}}{\sqrt{2}m} \\ -\frac{iP\hbar k_{lp}}{m} & \varepsilon_{va}^0-E & 0 \\ -\frac{iP\hbar k_{lp}}{\sqrt{2}m} & 0 & \varepsilon_{soa}^0-E \end{vmatrix}=0, \tag{26}$$

$$\begin{vmatrix} \varepsilon_{cb}^0 \pm x\langle S_z\rangle(N_0\alpha) - E & \frac{P\kappa_{lp}^{\pm}}{m} & \frac{P\kappa_{lp}^{\pm}}{\sqrt{2}m} \\ -\frac{P\kappa_{lp}^{\pm}}{m} & \varepsilon_{vb}^0 + \delta\varepsilon_v \pm \frac{x}{6}\langle S_z\rangle(N_0\beta) - E & \mp\frac{x\sqrt{2}}{3}\langle S_z\rangle\frac{(N_0\gamma)+(N_0\beta)}{2} \\ -\frac{P\kappa_{lp}^{\pm}}{\sqrt{2}m} & \mp\frac{x\sqrt{2}}{3}\langle S_z\rangle\frac{(N_0\gamma)+(N_0\beta)}{2} & \varepsilon_{sob}^0 + \delta\varepsilon_{so} \pm \frac{x}{6}\langle S_z\rangle(N_0\gamma) - E \end{vmatrix} = 0. \quad (27)$$

The bulk wave vectors of the heavy holes in the well and barriers are determined, respectively, by the equations

$$\varepsilon_{va}^0 + \frac{\hbar^2 k_{hh}^2}{2m_{hh}} - E = 0, \quad (28)$$

$$\varepsilon_{vb}^0 + \delta\varepsilon_v \mp \frac{x}{2}\langle S_z\rangle(N_0\beta) - \frac{\hbar^2 \kappa_{hh}^{\pm\,2}}{2m_{hh}} - E = 0. \quad (29)$$

Here the bare sp band energies for the well and barrier semiconductor are referred to as a and b, respectively. It follows from these dispersion relations that the quantum well states are split by the exchange potential at $\mathbf{k}_\perp = 0$ already. The time-reversal degeneracy of the energy levels is lifted because of the spin-orbit interaction. The explicit form of the wave functions written in the first order of perturbation theory shows that the average spin vectors $\langle \Psi^{\pm}|\mathbf{\Sigma}|\Psi^{\pm}\rangle$ ($\mathbf{\Sigma}$ is the spin operator) for these split-off states have opposite directions.

These results will now be applied to the quantum well $Cd_{1-x}Mn_xTe/CdTe/Cd_{1-x}Mn_xTe$ as an extensively studied magnetic structure. We take the temperature as $T=0$. As input parameters of the bulk constituents we use the values given in Ref. 25. They were obtained in the virtual crystal approximation in which a zinc blende MnTe was considered as a hypothetical crystal.[27] The parameters used are presented in Table I. Leaving the problem of the exact value of the valence-band offset Λ beyond this paper we examine magnetic quantum wells with offsets in the interval 25–100 meV. The well width varies within the limits 20–100 Å. It is worth noting that the exchange parameters $(N_0\beta)$ and $(N_0\gamma)$ calculated by formulas (20) with the characteristic parameters give the values of -0.879 and -0.971 eV, respectively, which are in very good agreement with the experimental data as the mean-field approach gives $(N_0\beta)\sim(N_0\gamma) = -0.88$ eV (Ref. 27).

TABLE I. Bulk $\mathbf{k}\cdot\mathbf{p}$ and magnetic exchange parameters.

Parameter	CdTe	$Cd_{1-x}Mn_xTe$
$\varepsilon_c^0 - \varepsilon_v^0$ (eV)	1.606	$1.606 + 1.592x$
$\varepsilon_v^0 - \varepsilon_{so}^0$ (eV)	0.94	$0.94 - 0.1x$
$\varepsilon_v^0 - \varepsilon_d^0$ (eV)		3.4
m_{hh}/m_0	0.4	0.6
$2m_0P^2$ (eV)	20	20
U (eV)		7.0
V_{pd} (eV)		0.49
$(N_0\alpha)$		0.22

In the framework of the developed model, the energy levels and their wave functions as a function of the polarization parameter y and the well width L have been calculated for different magnitudes of the valence-band offset parameter Λ and the fraction x of manganese cations. Figures 2, 3 show the spin splitting effect of the light particle and heavy hole states of the magnetic quantum well structure $Cd_{1-x}Mn_xTe/CdTe/Cd_{1-x}Mn_xTe$ with $x=0.1$ for two values of the well width $L=100$ (a) and 20 Å (b). In this case the calculation was performed for $\Lambda=0.025$ eV. As follows from Fig. 2, when increasing the polarization P (or decreasing y in our case), the light particle energy levels with spin-up and spin-down split in opposite directions showing the spin-splitting effect. For the thick quantum well the effect reaches a magnitude of 10 meV at $y=0.4$. By decreasing the well width, the spin splitting effect increases substantially. In the case of $L=20$ Å, the effect is of the order 60 meV at $y=0.2$. As a matter of fact, the spin splitting of the quantum well states follows directly from the magnetic splitting of the constituent bulk bands. This is shown in Fig. 2(c), in which the Γ_6 bulk band diagram of the quantum well considered at $y=0.5$ (solid lines) and at $y=0.2$ (dashed and dashed-dotted lines) is presented. In the figure the interval $|z/L|<0.5$ corresponds to the well and $z/L>0.5$ corresponds to the barrier.

For the heavy holes (Fig. 3), the quantum well states with spin up and spin down are allowed to appear in the point $y=1/2$ only, in which the spectrum must be doubly spin degenerate. In the case of nonzero polarization the states with spin down survive but the spin-up modes are not permitted. This result is explained in Fig. 3(c) showing the shift of the Γ_8 heavy hole bulk band of the constituents in the unpolarized case ($y=0.5$) and in the case of the nonzero polarization ($y=0.2$). In Fig. 3(a) the ground states for the even and odd modes are shown by the dashed lines while the excited states are shown by the dotted lines. We note that the excited states appear for some non-zero values of the polarization in this case, being states with spin down.

The spin-splitting effect for the magnetic quantum well with the fraction of the manganese ions $x=0.2$ and the valence bands offset $\Lambda=0.1$ eV is shown in Fig. 4. The trend of the light particle quantum well states are similar to the previous structure in consequence of the similar band diagram of the bulk Γ_6 band edge for these two quantum wells.

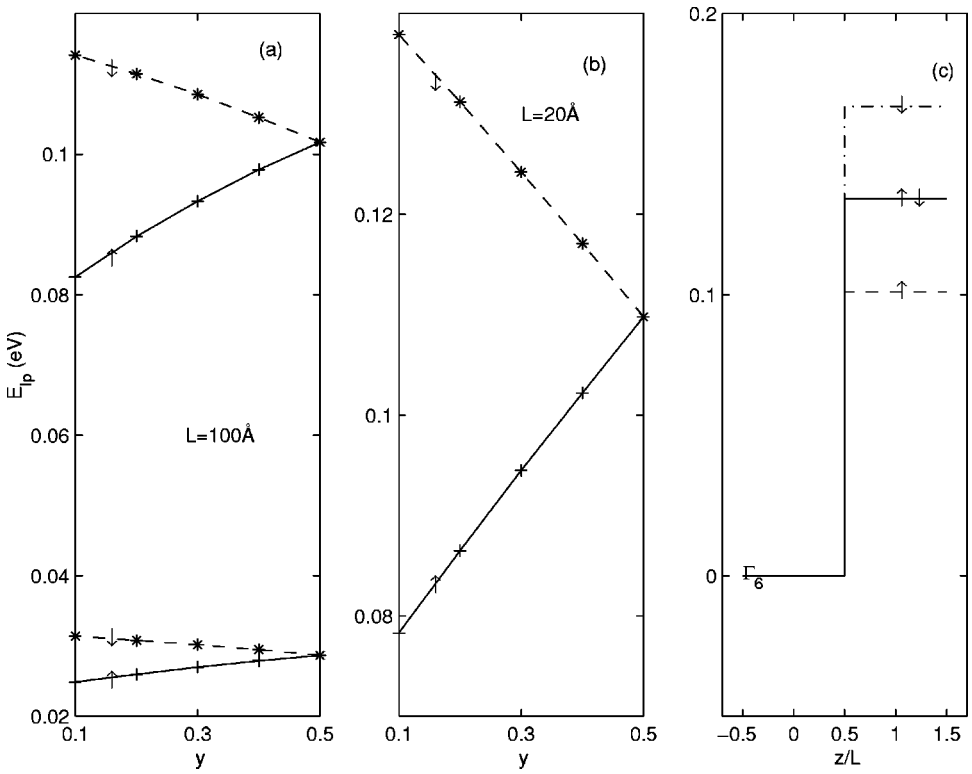

FIG. 2. Spin-splitting effect for the light particle lowest states of the magnetic quantum well $CdTe/Cd_{1-x}Mn_xTe$ ($x=0.1$, $\Lambda=0.025$ eV) with the well width (a) $L=100$ Å and (b) 20 Å. The trend for the states with spin up (down) is shown by solid (dashed) lines, the calculated points being marked by the crosses (stars). (c) The Γ_6 conduction bulk band diagram of the quantum well for $y=0.5$ and $y=0.2$ is shown by solid lines and by dashed lines, respectively. $|z/L|<0.5$ corresponds to the well and $(z/L>0.5)$ corresponds to the barrier.

So, we do not present this figure here. In contrast, the heavy hole quantum well states exhibit quite different behavior (Fig. 4). When decreasing y down to $y=0.4$, the energy of states with spin up increases but for the states with spin down it decreases. The splitting of the energy levels reaches ~ 10 meV in the case of $L=100$ Å, and for the larger values of the polarization the state with spin up is pushed out of the well. As a result only the state with spin down can exist in the quantum well. The explanation of this follows directly from the band diagram shown in Fig. 4(c).

The characteristic form of the envelope wave functions of the light particle main even mode, for the magnetic quantum well with $x=0.1$, $\Lambda=0.025$ eV and $L=100$ Å is shown in Fig. 5. The spin-splitting effect for this mode was presented

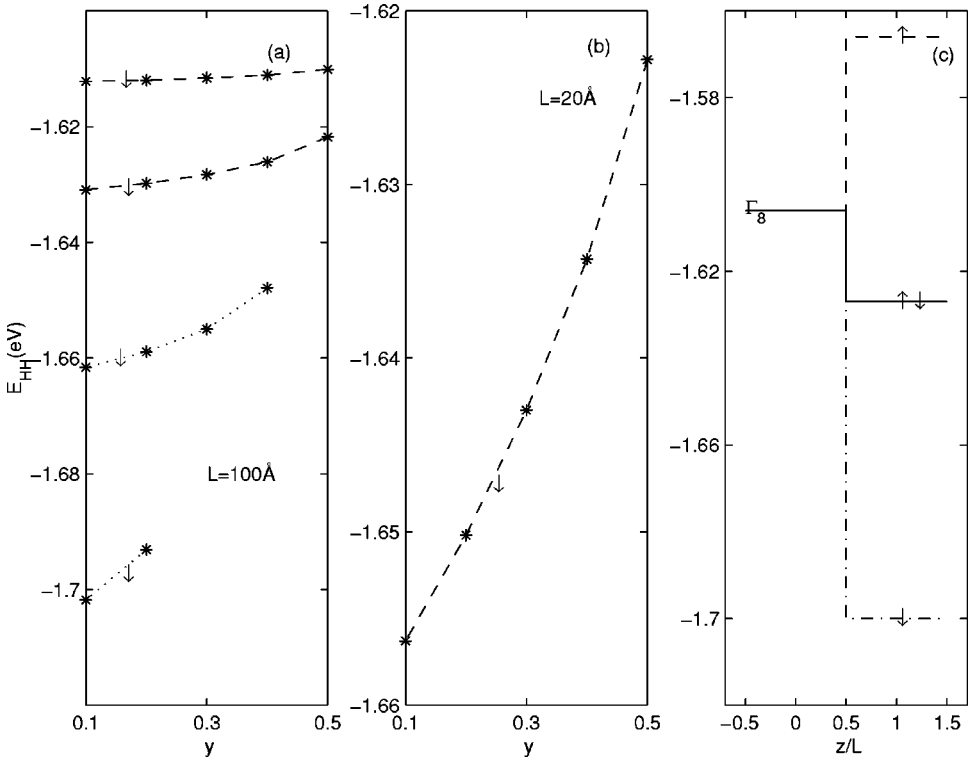

FIG. 3. Spin-splitting effect for the lowest heavy hole states of the magnetic quantum well $CdTe/Cd_{1-x}Mn_xTe$ ($x=0.1$, $\Lambda=0.025$ eV) with the well width (a) $L=100$ Å and (b) 20 Å. The trend for the states with spin up (down) is shown by solid (dashed) lines, the calculated points being marked by the crosses (stars). The dotted lines show the appearance of excited states for the nonzero spin polarization. (c) The Γ_8 heavy hole bulk band diagram of the quantum well in the case of $y=0.5$ (solid lines) and $y=0.2$ (dashed lines). $|z/L|<0.5$ corresponds to the well and $(z/L>0.5)$ corresponds to the barrier.

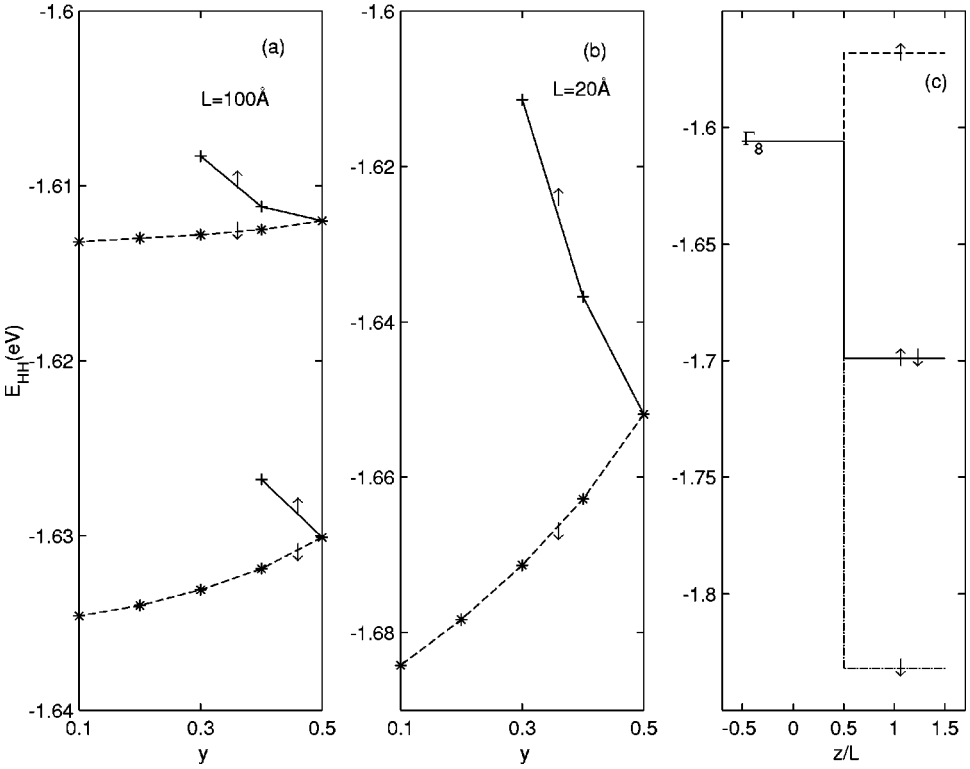

FIG. 4. The same as in Fig. 3, but for the quantum well with $x=0.2$, $\Lambda=0.1$ eV.

in Fig. 2. The form of the envelope wave functions does not change with polarization dramatically, because only the tails feel the presence of the Mn atoms in the barriers. This important distinction between quantum well structures with either Mn-based wells or barriers has been first discussed by Egues and Wilkins in Ref. 34.

IV. DISCUSSION

In our approach the magnetic semiconductor alloy has been presented in the form $A^{\mathrm{II}}_{1-x}\mathrm{Mn}^{\uparrow}_{xy}\mathrm{Mn}^{\downarrow}_{x(1-y)}B^{\mathrm{VI}}$, the parameter y indicating the magnitude of the polarization of the magnetic atoms. It may be changed, for example, by an external magnetic field or by the temperature. The relation be-

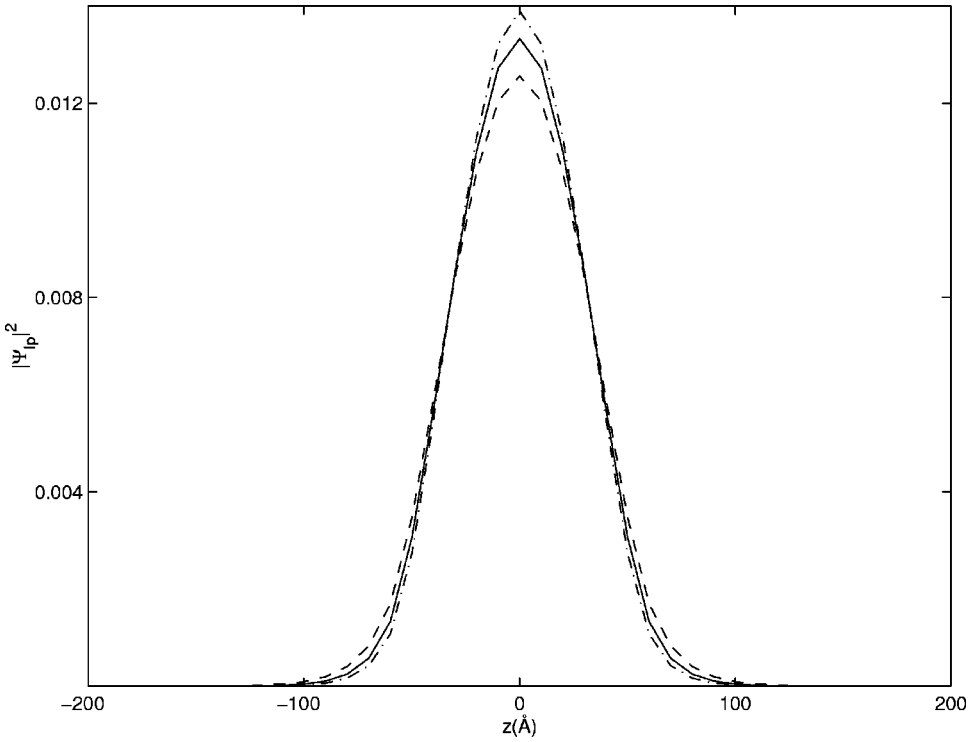

FIG. 5. The envelope wave functions of the light particle main even mode, for the magnetic quantum well with $x=0.1$, $\Lambda=0.025$ eV, and $L=100$ Å. The spin-splitting effect for this mode was presented in Fig. 2(a). The envelope wave functions for the unpolarized case is shown by the solid line, those for states with spin up and down at $y=0.2$ are shown by dashed and dotted lines, respectively.

tween the parameter y and the magnetic field can be obtained from the definition of the average value of the Mn spins $\langle S_z \rangle = \frac{5}{2}(2y-1)$ in this approach and its expression in the molecular field theory[35] $\langle S_z \rangle = -\frac{5}{2} B_{5/2}(\xi)$. Here $B_{5/2}$ is the standard Brillouin function with $\xi = \frac{5}{2} g_{Mn} \mu_B B/(k_B T)$, where g_{Mn} is the Lande factor for Mn. The Brillouin function goes to unity for large magnitudes of the argument and for small ξ it is approximately a linear function. For example, the value $y=0.48$ corresponds to the magnitude of the field $B_z = 2$ T at the temperature $T=2$ K.

The quantum wells have been considered in the flat band approximation, so band bending effects have been neglected. But we keep in mind that the band bending effect will be important in thick modulation-doped quantum wells based on II-VI semiconductors. This problem is left to be studied in a future publication. We neglected in this work strain effects, motivating this step, at first, by the good lattice match of the systems $Cd_{1-x}Mn_xTe/CdTe$ (the lattice mismatch is about 0.6 %). Moreover, the band-edge magnetic splittings, one of the most interesting features of these structures, are not affected appreciably by strain. However, strain effects can be easily included in the Hamiltonian, but they mainly give corrections to the diagonal terms leading to the trivial shifts of the levels. We have also restricted ourselves to the band-edge splitting effect leaving the in-plane dispersion of the spin-split quantum well states out of our consideration in this work. But it is worth noting that the developed model can be extended to include the $k_\perp$ terms and construct an effective Luttinger Hamiltonian. An alternative and elaborate development of the Luttinger model for the magnetic semiconductors has been given recently in Ref. 36. But according to our preliminary results by symmetry the model Hamiltonian obtained in this Ref. 36 and in our model turned out to be in close agreement.

The numerical results obtained are in reasonable accord as with the experimental data[37,38] and with other theoretical models.[37,39] The experimental measurements of the magnetoabsorption of the ferromagnetic $Ga_{1-x}Mn_xAs$ epilayers presented in Ref. 38 give a magnitude of the spin-splitting of the order 10 meV for a magnetic field ~ 5 T, the splitting closely following the magnetization of the epilayers. This fact agrees reasonably with the numerical results shown in Figs. 2–4, supporting the common trends of the energy levels with the polarization. Other experimental measurements of the photoluminescence excitation spectroscopy of the CdTe/(Cd,Mn)Te quantum wells[37] agreed with our numerical data very well. A self-consistent model of the spin-polarized magnetic semiconductor quantum wells has been suggested in the recent Ref. 39 on the basis of a one-band Hamiltonian. The magnitudes and general trends of the splitting effect give additional support for the above approach.

V. SUMMARY

An effective model of magnetic semiconductor structures based on the II-VI semiconductors has been developed. In the first approximation of perturbation theory the model can be reduced to an empirical eight-band Kane model. In this simplest approach the model allows us to get analytical solutions and to follow the generation of the physical effects.

In the framework of the developed model the spin-splitting effect of the magnetic quantum well structures $Cd_{1-x}Mn_xTe/CdTe/Cd_{1-x}Mn_xTe$ has been studied in some detail. All the structures studied show the essential spin splitting effect which can be changed by the polarization (or by the magnetic field) and by the width of the well. At zero polarization ($y=1/2$) all the levels are doubly degenerate because of the time reversal symmetry of the structure. When including the polarization the levels split by the sp-d hybridization. The states with opposite average spin directions are shifted in energy in opposite directions. The splitting increases with increasing polarization and with decreasing well width L. The generation of the energy shifts of the quantum well states follows directly from the analysis of the bulk energy spectrum of the constituents. If for some values of y the polarization effect is larger than the energy offset (the overlapping between the bulk bands of the constituents) then the level with a certain spin direction is not permitted and disappears. As a result, it is possible to have the situation in a magnetic quantum structure where only states with one spin direction can exist. Thus even if there is only partial spin polarization in the semimagnetic barriers we can have complete spin polarization of bound states in the nonmagnetic quantum wells. What is most important is that this situation can be easily controlled by the choice of the constituent semiconductors and by the magnetic field. We point out that this effect is very closely related to the spin polarized transport problem.

The good agreement between the experimental and theoretical data encourages us to conclude that the theoretical model of the magnetic semiconductor structures developed in this work can be used to interpret the experimental results and to predict new physical effects relevant to spin electronic problems.

ACKNOWLEDGMENTS

One of the authors (N.M.) wishes to acknowledge the support of the Swedish Institute and to thank the Laboratory of Photonics and Microwave Engineering, Department of Microelectronics and Information Technology of the Royal Institute of Technology for its kind hospitality during this work. We are grateful to Professor Matsukura for the kindly presented preprint of Ref. 36 prior to publication.

[1] M. von Ortenberg, Phys. Rev. Lett. **49**, 1041 (1982).
[2] N. Dai, H. Luo, F. C. Zhang, N. Samarth, M. Dobrowolska, and J. K. Furdyna, Phys. Rev. Lett. **67**, 3824 (1991).
[3] W. C. Chou, A. Petrou, J. Warnock, and B. T. Jonker, Phys. Rev. Lett. **67**, 3820 (1991).
[4] G. A. Prinz, Phys. Today **48**, 58 (1995).
[5] S. Datta and B. Das, Appl. Phys. Lett. **56**, 665 (1990).
[6] P. R. Hammar, B. R. Bennett, M. J. Yang, and M. Johnson, Phys.

Rev. Lett. **83**, 203 (1999).
[7] G. Schmidt, D. Ferrand, L. W. Molenkamp, A. T. Filip, and B. J. van Wees, Phys. Rev. B **62**, R4790 (2000).
[8] M. Oestreich, J. Hübner, D. Hägele, P. J. Klar, W. Heimbrodt, W. W. Rühle, D. E. Ashenford, and B. Lunn, Appl. Phys. Lett. **74**, 1251 (1999).
[9] R. Fiederling, M. Kelm, G. Reuscher, W. Ossau, G. Schmidt, A. Waag, and L. W. Molenkamp, Nature (London) **402**, 787 (1999).
[10] Y. Ohno, D. K. Young, B. Beschoten, F. Matsukura, H. Ohno, and D. D. Awschalom, Nature (London) **402**, 790 (1999).
[11] J. C. Egues, Phys. Rev. Lett. **80**, 4578 (1998).
[12] Y. Guo, H. Wang, B. L. Gu, and Y. Kawaszoe, J. Appl. Phys. **88**, 6614 (2000).
[13] T. Hayashi, M. Tanaka, and A. Asamitsu, J. Appl. Phys. **87**, 4673 (2000).
[14] B. T. Jonker, Y. D. Park, B. R. Bennett, H. D. Cheong, G. Kioseoglou, and A. Petrou, Phys. Rev. B **62**, 8180 (2000).
[15] E. I. Rashba, Phys. Rev. B **62**, R16 267 (2000).
[16] E. A. de Andrada e Silva, G. C. La Rocca, and F. Bassani, Phys. Rev. B **50**, 8523 (1994).
[17] E. A. de Andrada e Silva, G. C. La Rocca, and F. Bassani, Phys. Rev. B **55**, 16 293 (1997).
[18] O. Mauritz and U. Ekenberg, Phys. Rev. B **55**, 10 729 (1997).
[19] G. Dresselhaus, Phys. Rev. **100**, 580 (1955).
[20] M. Silver, W. Batty, A. Ghiti, and E. P. O'Reilly, Phys. Rev. B **46**, 6781 (1992).
[21] Ya. A. Bychkov and E. I. Rashba, J. Phys. C **17**, 6039 (1984).
[22] M. Johnson, Phys. Rev. B **58**, 9635 (1998).
[23] N. Malkova and U. Ekenberg, Phys. Rev. B **66**, 155325 (2002).
[24] P. M. Hui, H. Ehrenreich, and K. C. Hass, Phys. Rev. B **40**, 12 346 (1989).
[25] P. M. Young, H. Ehrenreich, P. M. Hui, and K. C. Hass, Phys. Rev. B **43**, 2305 (1991).
[26] N. F. Johnson, H. Ehrenreich, P. M. Hui, and P. M. Young, Phys. Rev. B **41**, 3655 (1990).
[27] B. E. Larson, K. C. Hass, H. Ehrenreich, and A. E. Carlsson, Phys. Rev. B **37**, 4137 (1988).
[28] B. Velicky, J. Masek, G. Paolueci, V. Chab, M. Shurman, and K. C. Price in *Festkörperprobleme (Advances in Solid State Physics)*, edited by P. Grosse (Pergamon/Vieweg, Braunschweig, 1985), Vol. 25, p. 247.
[29] H. Ehrenreich, H. C. Hass, N. F. Johnson, B. E. Larson, and R. J. Lempert in *Proceedings of the 18th International Conference on Physics of Semiconductors*, edited by O. Engström (World Scientific, Singapore, 1987), p. 1751.
[30] However, the Ising type model can be applied for delute magnetic semiconductors only in the limit of small fraction of the magnetic atoms ($x<0.2$). A more accurate description should be based on a Heisenberg model. [See, for example, W. Y. Ching and D. L. Huber, Phys. Rev. B **26**, 6164 (1982)].
[31] G. Bastard, *Wave Mechanics Applied to Semiconductor Heterostructures* (Les Editions de Physique, Les Ulis, 1988).
[32] E. O. Kane, J. Phys. Chem. Solids **1**, 249 (1957).
[33] Note that we here refer to the parity of the total wave function, including the cell-periodic part of the wave function, which has odd parity. Thus the states referred to as even (odd) parity has an envelope function with odd (even) parity.
[34] J. C. Egues and J. W. Wilkins, Phys. Rev. B **58**, R16 012 (1998).
[35] J. Callaway, *Quantum Theory of Solid State* (Academic Press, New York, 1991).
[36] T. Dietl, H. Ohno, and F. Matsukura, Phys. Rev. B **63**, 195 205 (2001).
[37] S.-K. Chang, A. V. Nurmikko, J.-W. Wu, L. A. Kolodziejski, and R. J. Gunshor, Phys. Rev. B **37**, 1191 (1988).
[38] J. Szczytko, W. Mac, A. Twardowski, F. Matsukura, and H. Ohno, Phys. Rev. B **59**, 12 935 (1999).
[39] S. P. Hong, K. S. Yi, and J. J. Quinn, Phys. Rev. B **61**, 13 745 (2000).